Agent Based In-Situ Visualization by Guide Field

Yan Wang[a] and Akira Kageyama[b]
Graduate School of System Informatics, Kobe University, Kobe 657-8501, Japan

Keywords: High Performance Computing, In Situ Visualization, Agent Based Modeling.

Abstract: In situ visualization has become an important research method today in high performance computing. In our previous study, we proposed 4D Street View (4DSV), in which multiple visualization cameras are scattered in the simulation region for interactive analysis of visualization video files after the simulation. A challenge in the 4DSV approach is to increase the camera density around a local area of the simulation box for detailed visualizations. To make the cameras automatically identify such a local region or Volume of Interest (VOI), we propose introducing the concept of a swarm of visualization cameras, which is an application of agent-based modeling to in-situ visualization. The camera agents in the camera swarm are autonomous entities. They find VOIs by themselves and communicate with each other through a virtual medium called a visualization guide field that is distributed in the simulation space.

1 INTRODUCTION

The post hoc visualization is the standard way for scientific visualization today, especially in high-performance computing (HPC). A drawback of the post hoc visualization method is that it inevitably accompanies massive numerical data that is to be stored and transferred. On the other hand, the in-situ visualization (Childs et al., 2020) enables directly retrieving visualization images without going through massive numerical data (Bennett et al., 2018; Tikhonova et al., 2010a; Tikhonova et al., 2010b; Ye et al., 2013; Kawamura et al., 2016; Childs et al., 2022; Demarle and Bauer, 2021).

A challenge in in-situ visualization is compensating for its lack of interactivity. Here, interactivity means real-time control of visualization settings such as viewpoint position, viewing direction, and other parameters in terms of adopted visualization algorithms, e.g., the level of the isosurface. The visualization setting should be prescribed before a simulation starts in the in-situ visualization.

We proposed an in-situ visualization approach that enables interactive analysis, rather than interactive control, of the in-situ visualization setting though visualized video files (Kageyama and Yamada, 2014). The key idea is to apply multiple in-situ visualizations from many different viewpoints at once, then to apply the interactive exploration of the video dataset produced by the in-situ visualization. A similar image-based approach to in-situ visualization is Cinema (Ahrens et al., 2014; O'Leary et al., 2016). By generalizing our video-based method, we proposed "4D Street View (4DSV)" (Kageyama and Sakamoto, 2020; Kageyama et al., 2020), where we place thousands omnidirectional cameras having a full (=4π steradians) field of view. The viewpoint and viewing direction can then be changed interactively, like Google Street View (Anguelov et al., 2010), through a PC application called 4D Street Viewer.

In computer simulations, visualization is commonly applied intensively to only a tiny portion of the entire simulation space. We refer such a localized region as Volume of Interest (VOI) in this paper.

If the location and size of a VOI is known before the simulation starts, we can place the visualization viewpoints, or cameras, intensively around there. The phenomena occurring in the VOI can be analyzed interactively by the 4D Street Viewer. However, there are possible cases where the location and motion of a VOI is unpredictable.

A straightforward resolution for those cases is to increase the total number of visualization cameras, decreasing the distances between the cameras. We can perform 4DSV with $O(10^3)$ omnidirectional cameras with no problem (Kageyama and Sakamoto, 2020; Kageyama et al., 2020), but it is practically difficult to increase the camera number to $O(10^4)$, or

[a] https://orcid.org/0000-0001-7700-0998
[b] https://orcid.org/0000-0003-0433-668X

Wang, Y. and Kageyama, A.
Agent Based In-Situ Visualization by Guide Field.
DOI: 10.5220/0012092800003546
In *Proceedings of the 13th International Conference on Simulation and Modeling Methodologies, Technologies and Applications (SIMULTECH 2023)*, pages 332-339
ISBN: 978-989-758-668-2; ISSN: 2184-2841

more, because of computational costs.

This paper aims to propose a new method that allows 4DSV with high spatial camera density with relatively small number of visualization cameras, even for unpredictable VOI behaviors.

The concept of Agent Based Visualization (ABV) was proposed in 2017 (Grignard and Drogoul, 2017), which combines Agent Based Model (ABM) with information visualization in general. We proposed an applicaiton of ABV to in-situ visualization for HPC (Wang et al., 2022; Wang et al., 2023). In our agent-based in situ visualization method, the agents are visualization cameras that autonomously identify and track VOIs by following prescribed simple rules and applying in situ visualization.

Only the case of a single autonomous camera tracking the motion of an unpredictable VOI was shown in the previous work. As a natural extension, we propose a method where multiple camera agents follow multiple VOIs, in this paper. The challenges here are the followings: (i) An agent should pick out the closest VOI among multiple VOIs and get closer to the VOI; (ii) the agent should track the VOI motion with keeping an appropriate distance for visualization; and (iii) agents that track the same VOI should maintain an appropriate mutual distance each other so as not to apply visualization of the same VOI from almost the same viewpoint.

In short our approach incorporates the intelligence of a swarm into camera agents for in-situ visualization. According to our process, camera agents can autonomously communicate with each other and the environment and other camera agents to determine the location of VOI and acquire VOI-related images, allowing a limited number of camera agents to acquire more critical information about the simulated environment.

In Section 2, we introduce the idea of agent-based modeling (ABM) and the technical details of this method. In Section 3, we perform test calculations to verify the feasibility of the method proposed in this paper. And Section 4 concludes this paper.

2 METHOD

2.1 Agent Motion

Generally, ABM consists of two parts; environment and agents (Wilensky and Rand, 2015). According to prescribed rules, each agent interacts with the environment and other agents.

Our proposed method considers multiple visualization viewpoints as a swarm of agents (Beni and Wang, 1993). Rules for the camera agents are designed to track multiple VOIs efficiently as a group (Dorigo and Blum, 2005).

The environment for the camera agents is a vector field called Visualization Guide Field (VGF) that corresponds to the pheromones used in ABM for ant colony (Dorigo and Blum, 2005; Deneubourg et al., 1990; Tisue and Wilensky, 2004). Each agent moves toward the VGF vector at its position; the VGF mediates all interactions between VOI and agents as well as among the agents.

We solve Newton's equation of motion for each agent, assuming that agents have unit mass. The force acting on the agents is a function of position determined by the VGF. Additional drag force proportional to the agent velocity is also introduced to damp high-frequency oscillations.

Agents should have two essential traits. First, they should move toward a nearby VOI. Second, they should keep an appropriate distance from each other.

To achieve the dual goals, we exploit the analogy of the electrostatic field: The VOI has a positive electric charge $+Q > 0$, and the agents have a negative charge $-q < 0$, where $Q > q$.

A negatively charged camera agent is attracted to the positively charged VOI, and the camera agent visualizes the VOI in detail from close up. The negatively charged camera agents are repelled by each other, so they avoid the waste of being located in the same place to visualize the same position.

The interaction between the VOI and the camera agent is unilateral. The agent changes its position due to the electric field caused by the VOI's positive charge, but the VOI is not affected by agents even if it is closely located. In other words, the "real space" in which the simulation is going on and the "virtual space" in which the agents reside share the space-time, but the interaction is one-way from the real space to the virtual space.

We can regard the electric potential of the VGF's electric field corresponds to the pheromone used ABMs (Deneubourg et al., 1990) in general.

The location of VOIs is specified in the simulation program in this work. The main purpose of VGF is to attract camera agents to the specified location of VOI. Negatively charged camera agents are automatically attracted to the positive VOI. When there are two or more VOIs, the VGF is given by the superposition of fields generated by each VOI. Since VGF decays as a function of radius in the inverse square law, an agent is attracted naturally toward the nearest VOI.

The spherically symmetric VGF generated by a positively charged VOI is useful when the VOI should be visualized from a point near the VOI from any an-

gle. But there are cases when some VOI should be visualized from a certain angle and the angle is known in the simulation. For example, in a fluid simulation in which vortex-rings are spontaneously formed. The VOI in this case can be specified in the simulation program as the local region where the enstrophy is spatially localized. The ring formation is detected by the distribution of the enstrophy density in the simulation. In those cases, camera agents should be attracted to the VOI, along the axis of the ring in order to get a better visualization of the ring formation process.

In order to guide the camera agents along a prescribed direction, we introduce a dipole-type field as a VGF. The spherically symmetric VGF is called monopole-type VGF.

In short, there are two types of VOI; monopole VOI and dipole VOI. A monopole VOI is a spherically distributed electric charge density with a net positive charge whose origin is the center of the VOI. A dipole VOI is a dipolar distribution of electric charge density whose moment vector is in the direction parallel to the appropriate view-direction for the in-situ visualization.

2.2 Visualization Guide Field

2.2.1 Spherical Double Layer: General Case

The dipole electric field by a point charge has a singular behaviour near $r = 0$. It has infinitely strong electric field near the point. In addition, we want the camera agents to keep a proper distance from the VOI center at $r = 0$. Because of these reasons, we realize the monopole electric field outside a specific radius by assuming an inner structure of charge density distribution in the sphere.

Suppose the center of VOI, $\mathbf{x}$, is at the origin, i.e., $\mathbf{x} = 0$, and the radius of the VOI is b. We assume a doubly layered spherical shell with the radii $r = a$ and $r = b$. We set a uniform negative charge density $-\rho_0$ in a sphere of radius a, i.e., for radius r with $0 \leq r \leq a$, and we set a uniform positive charge density $+\rho_0$ in the spherical shell $a < r \leq b$. We assume the permeability ε_0 in the SI unit system is 1.

Applying the Gauss' divergence theorem to the relationship between the electric field $\mathbf{E}$ and the charge density ρ, i.e., $\nabla \cdot \mathbf{E} = \rho$,

$$\int_S \mathbf{E} \cdot \mathbf{r}\, dS = \int \rho\, dV. \tag{1}$$

Due to the spherical symmetry of the system, the electric field $\mathbf{E}$ caused by the spherically distributed charge density has only the radial component E_r, i.e., $\mathbf{E} = E_r(r)\,\hat{\mathbf{r}}$, where $\hat{\mathbf{r}}$ is the radial unit vector.

The radial component is given as

$$E_r(r) = \begin{cases} -\frac{Q_a}{4\pi a^3} r & (0 < r \leq a) \\ \frac{Q_a}{4\pi a^3}\left(r - \frac{2a^3}{r^2}\right) & (a < r \leq b) \\ \frac{Q_a}{4\pi a^3}\frac{b^3 - 2a^3}{r^2} & (b \leq r). \end{cases} \tag{2}$$

Here

$$Q_a = \frac{4\pi a^3}{3}\rho_0 \tag{3}$$

is the total amount of charge in the sphere of $r \leq a$ if constant positive charge $+\rho_0$ is uniformly distributed. In fact, since $-\rho_0$ is distributed, the total amount of charge in the sphere of $r \leq a$ is $-Q_a$. The ratio of the two radii $r = a$ and $r = b$ determines the total charge in the sphere $r \leq b$ and therefore the sign of the electric field $E_r(r)$ outside the sphere $r > b$. If $b > b_0$, then $E_r(r) > 0$ for $r \geq b$, where

$$b_0 = \sqrt[3]{2}\, a \sim 1.260\, a \tag{4}$$

Integrating eqs. (2), we get the potential ϕ of this electric field as

$$\phi(r) = \begin{cases} \frac{\rho_0}{6} r^2 - \rho_0 a^2 + \frac{\rho_0}{2} b^2 + c_0 & (0 \leq a) \\ -\frac{\rho_0}{3}\left(\frac{r^2}{2} + \frac{2a^3}{r}\right) + \frac{\rho_0}{2} b^2 + c_0 & (a \leq r < b) \\ \frac{\rho_0}{3}\left(\frac{b^3 - 2a^3}{r}\right) + c_0 & (b \leq r) \end{cases} \tag{5}$$

where c_0 is the integration constant.

2.2.2 Electric Field of Monopole VOI

Because there is no particular rule to determine the value of b, we set $b = b_1$ for the monopole VOI with

$$b_1 = \sqrt{2}\, a \sim 1.414\, a \tag{6}$$

The potential at the origin $\phi(0) = 0$ with this b, see eq. (2). The charge density distribution for the monopole VOI is schematically shown in Fig. 1.

For later convenience, we explicitly write the radial electric field of the monopole-type VOI as $\mathbf{E}^{\mathrm{m}}$ with $b = b_1$ in eqs. (2):

$$E_r^{\mathrm{m}}(r) = \begin{cases} -\frac{Q_a}{4\pi a^3} r & (0 < r \leq a) \\ \frac{Q_a}{4\pi a^3}\left(r - \frac{2a^3}{r^2}\right) & (a < r \leq b_1) \\ \frac{Q_a}{4\pi}\frac{\alpha}{r^2} & (b_1 \leq r) \end{cases} \tag{7}$$

where

$$\alpha = 2^{\frac{3}{2}} - 2 \sim 0.828 \tag{8}$$

The function $E_r^{\mathrm{m}}(r)$ is monotonically decreasing for $0 < r \leq a$, monotonically increasing for $a < r \leq b_1$, and monotonically decreasing for $b_1 < r$. $E_r^{\mathrm{m}}(b_0) = 0$.

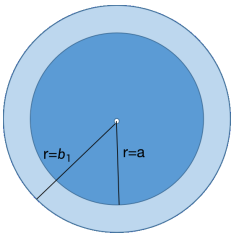

Figure 1: Schematic figure for the charge density distribution of monopole-type VOI. The white dot is in the center of the VOI, located at the origin of the two circles. The dark blue circle with radius a has a uniform distribution of negative charges; the light blue circle between radius a and radius b_1 has a uniform distribution of positive charges, which attracts the camera agent with a negative charge.

2.2.3 Electric Field of Dipole-Type VOI

The monopole VOI attracts camera agents, which are negatively charged, and make them apply in-situ visualization from all directions around the VOI's center.

There are cases when visualizations should be applied from a specific direction and the direction is known from the simulation program. To lead the camera agents toward the desired position near the VOI's center to apply the in-situ visualization from the desired direction, we introduce a dipole-type VOI. The key idea is to make an electrical dipole field outside a sphere $r = b_1$. The field-lines of the dipole field guide the negatively charged camera agents along the curved lines. The camera agents are naturally lead to the positive pole of the VOI's dipole.

As in the case of the monopole VOI, the pure dipole causes numerical trouble due to the singular behavior with rapidly increasing values near the origin $r = 0$. To avoid the problem, we introduce inner structure inside the sphere of $r = b_1$.

The potential of the dipole field with dipole moment $\mathbf{p}$ is (under the assumption of $\varepsilon_0 = 1$),

$$\frac{1}{4\pi}\frac{\mathbf{p}\cdot\mathbf{r}}{r^3} \tag{9}$$

which decays as a function of distance r as r^{-3} for $b_1 \le r$. This is different from the r^{-2} dependence of the radial electric field of monopole type VOI. The difference causes an undesired behavious of a camera agent; it can be more strongly attracted by a monopole VOI than by a dipole VOI even the latter is closer to the former. In order to release the difference of the r-dependency, we use the following "quasi-dipole" potential,

$$\tilde{\phi}(\mathbf{r}) = \frac{1}{4\pi}\frac{\mathbf{p}\cdot\mathbf{r}}{r^2} \tag{10}$$

We adopt the quasi-dipole electric field $\mathbf{E} = -\nabla\tilde{\phi}$ in $r < b_1$.

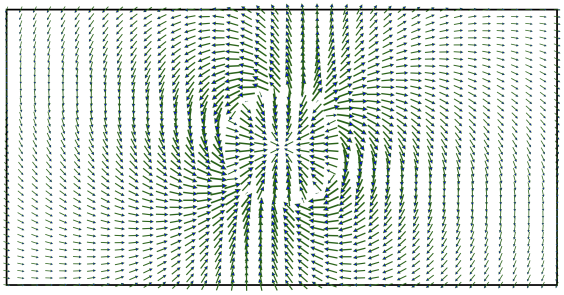

Figure 2: The electric field distribution around the dipole VOI.

$$\tilde{\mathbf{E}}(\mathbf{r}) = -\frac{1}{4\pi r^2}\left(\mathbf{p} - \frac{2(\mathbf{p}\cdot\mathbf{r})}{r^2}\mathbf{r}\right) \tag{11}$$

for $b_1 \le r$ which decays as r^{-2}.

As for the electric field inside the sphere of $r = b_1$, we smoothly connect the dipole field outside $r \ge b_1$ and a monopole-type electric field inside $r \le b_0$.

To put more precisely, we assume the radial electric field by a spherical double layer of eq. (2) with $b = b_0$.

$$E_r^{\mathrm{d}}(r) = \begin{cases} -\frac{Q_a}{4\pi a^3} r & (0 < r \le a) \\ \frac{Q_a}{4\pi a^3}\left(r - \frac{2a^3}{r^2}\right) & (a < r \le b_0) \end{cases} \tag{12}$$

Note that $E_r(r) = 0$ for $r > b_0$ in this case of $b = b_0 = \sqrt[3]{2}$.

In the intermediate layer of $b_0 < r \le b_1$, we assume the dipole field of eq. (11) with an attenuation factor

$$H(r) = \frac{r - b_0}{c - b_0} \tag{13}$$

as

$$\mathbf{E}(\mathbf{r}) = H(r)\tilde{\mathbf{E}}(\mathbf{r}) \tag{14}$$

in order to smoothly decay the dipole field toward zero at $r = b_0$.

In summary, the electric field of a (quasi-)dipole-type VOI with pseudo-dipole moment $\mathbf{p}$ placed at the origin is given by

$$\mathbf{E}^{\mathrm{d}}(\mathbf{r}) = \begin{cases} -\frac{Q_a}{4\pi a^3} r & (0 < r \le a) \\ +\frac{Q_a}{4\pi a^3}\left(r - \frac{2a^3}{r^3} r\right) & (a < r \le b_0) \\ -H(r)\frac{1}{4\pi r^2}\left(p - \frac{2(p\cdot r)}{r^2} r\right) & (b_0 < r \le b_1) \\ -\frac{1}{4\pi r^2}\left(p - \frac{2(p\cdot r)}{r^2} r\right) & (b_1 \le r) \end{cases} \tag{15}$$

The electric field distribution around the dipole VOI is shown in Fig. 2, each arrow denotes the direction of the electric field.

2.2.4 Multiple VOIs

In simulation in general, multiple VOIs could appear for in-situ visualizations. Suppose we place n_{m} monopole VOIs and n_{d} dipole VOIs. We denote VOI radius a_i and the center position x_i for i-th VOI ($i = 1,2,\ldots,n_{\mathrm{m}}$). and the same for the dipole VOIs.

The relative position vector from the VOI center to a point in the space is given by

$$\mathbf{r}_i = \mathbf{x} - \mathbf{x}_i, \tag{16}$$

with the distance

$$r_i = |\mathbf{r}_i|, \tag{17}$$

and unit vector

$$\hat{\mathbf{r}}_i = \frac{\mathbf{r}_i}{r_i}. \tag{18}$$

As in the case of the real electric field, we assume the linearity, or superposition principle, of the electric fields generated by multiple VOIs.

The electric field for a camera agent at the position $\mathbf{x}$ is given by the supoerposition of the monopole fields and dipole fields as,

$$\mathbf{E}(\mathbf{x}) = \sum_{i=1}^{n_{\mathrm{m}}} E_r^{\mathrm{m}}(r_i)\,\hat{\mathbf{r}}_i + \sum_{i=1}^{n_{\mathrm{d}}} E_r^{\mathrm{d}}(r_i)\,\hat{\mathbf{r}}_i \tag{19}$$

The computational cost of this VGF field is negligibly small.

3 TEST

We have performed test calculations to validate the visualization guide field (VGF) method described above. The purpose of these tests are to confirm the agents motion. Visualization by these camera agents are not considered here. Another note on these tests are on the dimension of the computation. In the derivations of the VGF, we assumed the 3-dimensional space. We validate this field on a plane in the 3D space on which the center of VOI is located. Assuming that all agents are on the same plane in the initial condition, we solve the motion of the agents only in this 2D plane.

The following test simulations are performed by PC and the simulation programs are written in Processing language.

3.1 Monopole VOI

Fig. 3 shows a sequence of snapshots of time development of camera agents when we place a monopole VOI at a fixed position. Multiple agents that are randomly distributed in the plane starts sensing the monopole-type VGF and moving toward the center of the monopole. The agents that were close to the monopole VOI evenly distribute it at the most suitable distance from the monopole VOI, i.e., around the circumference of radius b_0.

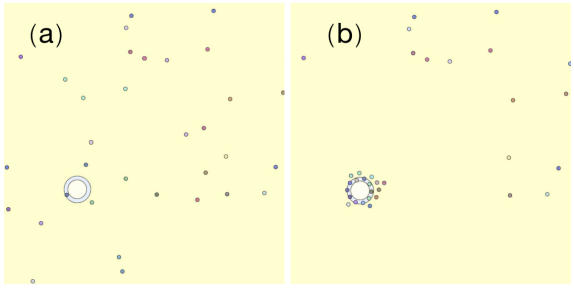

Figure 3: The motion of camera agents when a monopole VOI (large double circles with white and gray color) is fixed. (a) The original distribution of the camera agents.(b) The agents are uniformly located near the monopole VOI.

In order to check the track-ability of agents for moving monopole VOI, we place a moving VOI of the monopole type. The motion of the VOI is prescribed by combinations of sinusoidal functions of time in these tests.

Fig. 4 shows a time sequence from a period, the monopole VOI oscillates horizontally in this case. The camera agents that were initially distributed about the whole plane are attracted to the VOI and they follow a little behind the VOI as a group.

We have also performed tests in two dimensional monopole VOI motion, confirming that the agents can track the VOI motion as long as the VOI speed is not too high.

We also performed tests when the monopole VOI makes random movements. the camera agents can successfully find and track the monopole VOI as shown in Fig. 5.

3.2 Dipole VOI

Fig. 6 shows a snapshot when a dipole-type VOI is placed on the plane. The dipole moment is indicated by arrow in the VOI circle. The camera agents that were randomly distributed in the initial condition senses the dipole field and move along the field-line. They eventually accumulate around the “pole” of the dipole. This is the desired behaviour of the agents to realize the in-situ visualization of the VOI from a specific angle.

As shown in Fig. 7, when the dipole VOI does random motion, the camera agent can still detect and track the dipole VOI in time and can maintain a specific view of the dipole VOI.

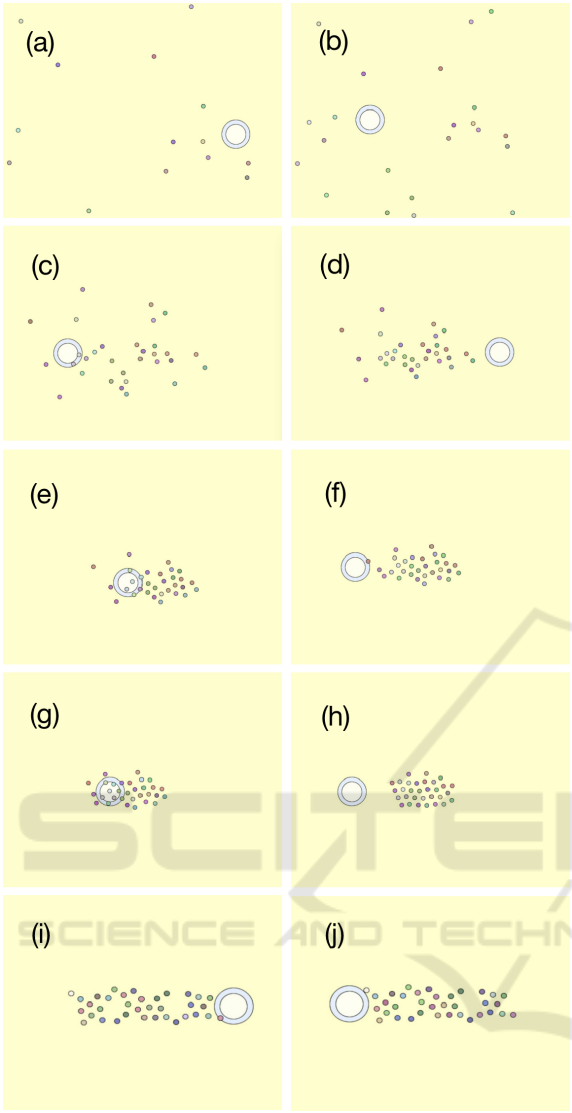

Figure 4: Camera agents when a monopole VOI is making a one-dimensional harmonic oscillation. (a) The original distribution of the monopole VOI and camera agents; (b) to (h) The camera agents gradually converging to the monopole VOI and following a little behind it as a group. (i) and (j) The camera agents successfully track the orbit of the VOI, but the lag becomes larger for a faster-moving VOI.

3.3 Multiple VOIs

The next experiment is to take into account how the camera agent will move when multiple monopole VOIs are present at the same time. As shown in Fig. 8, when three monopole VOIs appear at the same time, the camera agent will autonomously find the closest monopole VOI to it and follow it. As in the case of the single VOI case, the camera agents can follow the multiple VOIs even if they are moving. And, as the position of the monopole VOI changes, the camera agent can always choose to change the target to follow, tracking a closer VOI.

The final test shown is Fig. 9 in which a monopole VOI and a dipole VOI are present at the same time, the camera agents still find the closest VOI and tracks them autonomously.

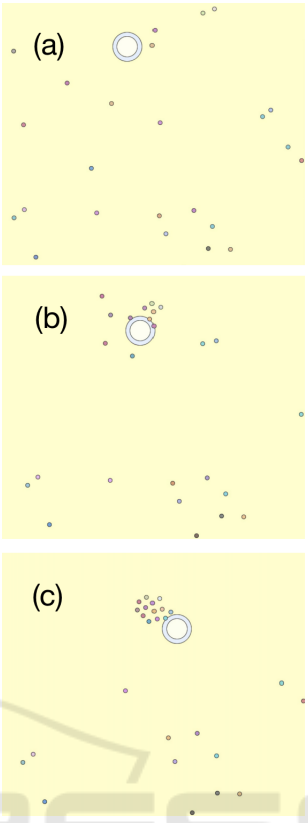

Figure 5: Camera agent when a monopole VOI makes random motion. (a) The original distributions; (b) Gradual aggregation of the camera agents toward the monopole VOI; (c) A part of the camera agents successfully follow the monopole VOI.

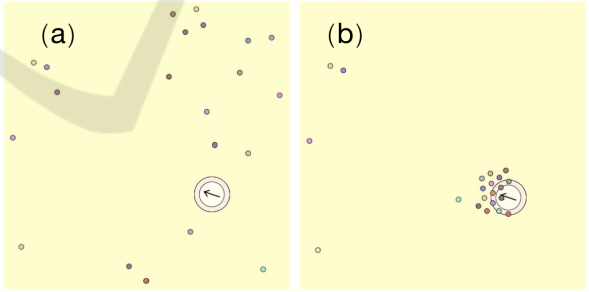

Figure 6: Camera agent when a dipole VOI is fixed. (a) The original distributions. (b) The agents are attracted to the dipole VOI from a specific direction.

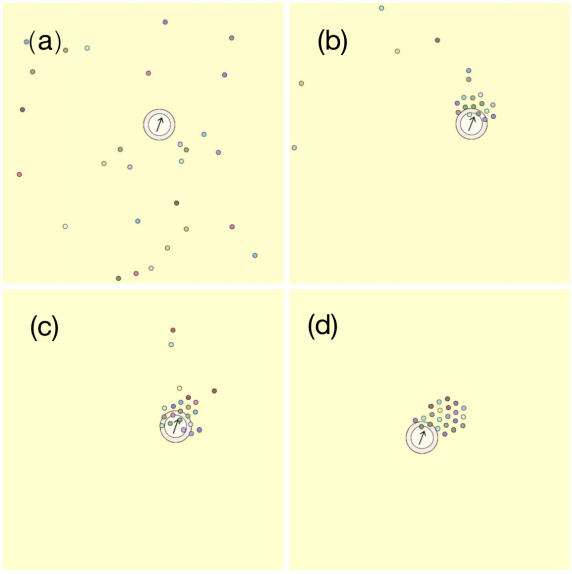

Figure 7: The camera agent when a dipole VOI does random motion. (a) The original distributions. (b) The camera agents converge near the dipole VOI from a specified direction. (c) The camera agents are aggregated in a suitable position, or the "pole", to observe the VOI from a proper viewing direction. (d) The agents continue to follow the VOI in motion.

4 CONCLUSIONS

We propose an agent based visualization approach to in-situ visualization for computer simulations. In this method, camera agents in a "camera swarm" communicate with each other and with the environment through a vector field, Visualization Guide Field (VGF).

The volume of interest (VOI) that should be applied intensive visualization is a source of VGF in our method. Inspired by the static electric field, a VOI that should be a focus of intensive visualization is a positively changed object and a visualization camera is a negatively charged object. The camera is a movable entity and called camera agent.

VOI can be either monopole-type or dipole-type. The monopole-type VOI corresponds to a local region where in-situ visualization should be applied in close-up, but from any direciton. The dipole-type VOI corresponds to a local region that should be visualized from a specific angle.

According to the repulsive force between agents, they can keep a proper distance even if they are attracted to the same VOI.

Our approach will improve the visualization efficiency by allowing camera agents to autonomously find and track VOI, reducing the number of cameras set up in the simulated environment and allowing us to obtain data focused on the region of interest rather than the background region.

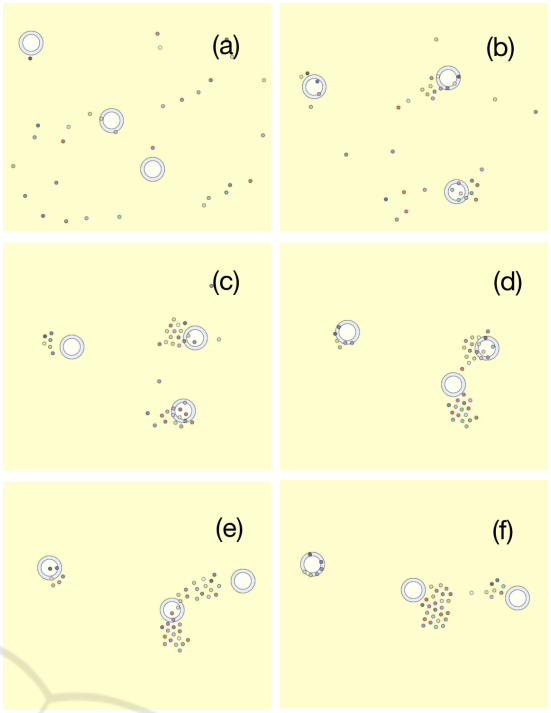

Figure 8: Motion of the camera agent when the monopole VOIs do random motion. (a) shows the original distribution of monopole VOI and camera agents; (b) shows that camera agents gradually converge to the nearest monopole VOI; (c) shows that camera agents will follow the monopole VOI motion after converging near their respective nearest monopole VOI. The colors of the camera agents are set randomly to facilitate observation, and different camera agents will select the closer monopole VOI for observation. (d),(e) show that the camera agents may also reselect the monopole VOI to be observed based on the distance after the monopole VOI motion produces an intersection. (f) shows that the camera agents will continue to steadily follow the selected monopole VOI after reselection.

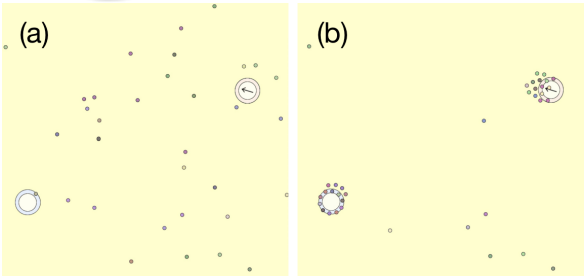

Figure 9: Motion of the camera agent when a monopole VOI and a dipole VOI are present at the same time. (a) shows the original distribution of VOIs and camera agents; (b) shows when camera agents are distributed around each VOI according to the demand of different VOIs.

ACKNOWLEDGEMENTS

This work was supported by JSPS KAKENHI (Grant Numbers 22H03603, 22K18703).

REFERENCES

Ahrens, J., Jourdain, S., O'Leary, P., Patchett, J., Rogers, D. H., and Petersen, M. (2014). An Image-Based approach to extreme scale in situ visualization and analysis.

Anguelov, D., Dulong, C., Filip, D., Frueh, C., Lafon, S., Lyon, R., Ogale, A., Vincent, L., and Weaver, J. (2010). Google street view: Capturing the world at street level. *Computer*, 43(6):32–38.

Beni, G. and Wang, J. (1993). Swarm intelligence in cellular robotic systems. In Dario, P. and others, editors, *Robots and Biological Systems: Towards a New Bionics?*, pages 703–712. Springer-Verlag Berlin Heidelberg.

Bennett, J. C., Childs, H., Garth, C., and Hentschel, B. (2018). In Situ Visualization for Computational Science. In *Situ Vis. Comput. Sci. Dagstuhl Semin. 18271*, volume 8, pages 1–43.

Childs, H., Ahern, S. D., Ahrens, J., Bauer, A. C., Bennett, J., Bethel, E. W., Bremer, P.-T., Brugger, E., Cottam, J., Dorier, M., Dutta, S., Favre, J. M., Fogal, T., Frey, S., Garth, C., Geveci, B., Godoy, W. F., Hansen, C. D., Harrison, C., Hentschel, B., Insley, J., Johnson, C. R., Klasky, S., Knoll, A., Kress, J., Larsen, M., Lofstead, J., Ma, K.-L., Malakar, P., Meredith, J., Moreland, K., Navrátil, P., O'Leary, P., Parashar, M., Pascucci, V., Patchett, J., Peterka, T., Petruzza, S., Podhorszki, N., Pugmire, D., Rasquin, M., Rizzi, S., Rogers, D. H., Sane, S., Sauer, F., Sisneros, R., Shen, H.-W., Usher, W., Vickery, R., Vishwanath, V., Wald, I., Wang, R., Weber, G. H., Whitlock, B., Wolf, M., Yu, H., and Ziegeler, S. B. (2020). A terminology for in situ visualization and analysis systems. *Int. J. High Perform. Comput. Appl.*, 34(6):676–691.

Childs, H., Bennett, J. C., and Garth, C., editors (2022). *In Situ Visualization for Computational Science*. Springer International Publishing.

Demarle, D. E. and Bauer, A. (2021). In Situ Visualization with Temporal Caching. *Comput. Sci. Eng.*, 23:25–33.

Deneubourg, J.-L., Aron, S., Goss, S., and Pasteels, J. M. (1990). The self-organizing exploratory pattern of the argentine ant. *J. Insect Behav.*, 3(2):159–168.

Dorigo, M. and Blum, C. (2005). Ant colony optimization theory: A survey. *Theor. Comput. Sci.*, 344(2-3):243–278.

Grignard, A. and Drogoul, A. (2017). Agent-Based visualization: A Real-Time visualization tool applied both to data and simulation outputs. In *The AAAI-17 Workshop on Human-Machine Collaborative Learning*, pages 670–675.

Kageyama, A. and Sakamoto, N. (2020). 4D street view: a video-based visualization method. *PeerJ Comput Sci*, 6:e305.

Kageyama, A., Sakamoto, N., Miura, H., and Ohno, N. (2020). Interactive exploration of the In-Situ visualization of a magnetohydrodynamic simulation. *Plasma and Fusion Research*, 15:1401065–1401065.

Kageyama, A. and Yamada, T. (2014). An approach to exascale visualization: Interactive viewing of in-situ visualization. *Comput. Phys. Commun.*, 185(1):79–85.

Kawamura, T., Noda, T., and Idomura, Y. (2016). In-situ visual exploration of multivariate volume data based on particle based volume rendering. In *2nd Work. Situ Infrastructures Enabling Extrem. Anal. Vis.*, pages 18–22.

O'Leary, P., Ahrens, J., Jourdain, S., Wittenburg, S., Rogers, D. H., and Petersen, M. (2016). Cinema image-based in situ analysis and visualization of MPAS-ocean simulations. *Parallel Comput.*, 55:43–48.

Tikhonova, A., Correa, C. D., and Kwan-Liu, M. (2010a). Explorable images for visualizing volume data. *Proc. IEEE Pacific Vis. Symp. 2010, PacificVis 2010*, pages 177–184.

Tikhonova, A., Correa, C. D., and Ma, K. L. (2010b). Visualization by proxy: A novel framework for deferred interaction with volume data. *IEEE Trans. Vis. Comput. Graph.*, 16(6):1551–1559.

Tisue, S. and Wilensky, U. (2004). NetLogo: Design and implementation of a multi-agent modeling environment. In *Proceedings of the Agent 2004 Conference on Social Dynamics: Interaction, Reflexivity and Emergence*.

Wang, Y., Ohno, N., and Kageyama, A. (2023). In situ visualization inspired by ant colony formation. *Plasma and Fusion Research*, 18:2401045.

Wang, Y., Sakai, R., and Kageyama, A. (2022). Toward agent-based in situ visualization. In By, C. and Choi, C., editors, *Methods and Applications for Modeling and Simulation of Complex Systems. CCIS*, 1636.

Wilensky, U. and Rand, W. (2015). *An Introduction to Agent-Based Modeling: Modeling Natural, Social, and Engineered Complex Systems with NetLogo*. MIT Press.

Ye, Y., Miller, R., and Ma, K.-L. (2013). In situ pathtube visualization with explorable images. In *13th Eurographics Symp. Parallel Graph. Vis.*, pages 9–16. Eurographics Association.